BIBECHANA
ISSN 2091-0762 (Print), 2382-5340 (Online)
Journal homepage: http://nepjol.info/index.php/BIBECHANA
Publisher: Department of Physics, Mahendra Morang A.M. Campus, TU, Biratnagar, Nepal

Study of star formation rate and metallicity of the low redshift (z < 0.02) dwarf galaxies

S. P. Gautam[1*], A. Silwal[2], N. Lamichhane[3], A. K. Jha[1], B. Aryal[1]
[1]Central Department of Physics, Tribhuvan University, Kirtipur, Nepal
[2]Patan Multiple Campus, Tribhuvan University, Lalitpur, Nepal
[3]Prithvi Narayan Campus, Tribhuvan University, Pokhara, Nepal
[*]E-mail: astrosujan@gmail.com

Article Information:
Received: January 1, 2021
Accepted: February 22, 2021

Keywords:
Dwarf galaxies
Star formation rate
Spectra
Hα measurement
SDSS

ABSTRACT

In this paper, we have presented an analysis of emission lines from two dwarf galaxies. We analyzed the strongest emission lines of wavelength ranging from 4100 Å to 6700 Å. Among these emission lines, Hα and OIII have the highest intensities with 113.09×10^{-17} erg/s/cm^2/Å and 142.12×10^{-17} erg/s/cm^2/Å in the galaxies SDSSJ222726.64+120539.8 and SDSSJ162753.47+482529.3, respectively. The Gaussian fit carried out in these emission lines showed the perfect fits with regression coefficient greater than 98 %, and full width half maximum (FWHM) of less than 4 Å. The line ratios calculated between Hα and Hβ for SDSSJ222726.64+120539.8 and SDSSJ162753.47+482529.3 were 2.78 and 2.85, respectively, suggesting that the galaxies are starburst galaxies. The measurement of the Hα line from both galaxies was then used to assess the rate of star formation. The star formation rate of the galaxies SDSSJ222726.64+120539.8 and SDSSJ162753.47+482529.3 was found to be 0.010 $M_\odot$ year^{-1} and 0.016 $M_\odot$ year^{-1}, respectively, indicating a low rate of star formation, and the emission line metallicity was derived using the Hα and NII line, which were measured to be 8.23 dex and 8.70 dex, respectively.

DOI: https://doi.org/10.3126/bibechana.v18i2.34067

1. Introduction

Galaxies evolve by colliding with their neighboring galaxies through the interaction of their environment. These collisions and mergers of galaxies due to induced gravitation has been the best-known fact about the evolutionary mechanism [1]. In extragalactic research, the pivotal question remains to find to what extent the properties of galaxies are regulated by the initial condition and environment. Indeed, it has been found that the

evolution of galaxies relies heavily on their environment [2].

In understanding the evolution of the universe, studying the star formation rate in the universe or the individual galaxies can be essential knowledge. But in extragalactic astronomy, assessing the star formation and birth of a star is a difficult task [3]. The importance of star formation bursts in the low mass galaxies was not unlocked until the modeling of blue galaxies and interacting systems [4]. Our primary objective is the study of galaxy formation and evolution is to gain insight into the interaction between the gaseous and stellar components of the galaxies. So, Dwarf galaxies with low surface brightness but gas-rich, low-mass, low-metallicity are ideal for studying the rate of star formation, as it may give us an understanding of how gases turned into a star within that system that might imitate the early universes [5]. In addition, due to a simpler dynamic and morphological system than spiral galaxies, dwarf galaxies are considered the ideal laboratory for studying the formation of stars within the low gas surface density domain along with lower rotational shear rates [6].

While dwarf galaxies have received less attention than spiral galaxies and elliptical galaxies, they may have more cosmological importance. These dwarf galaxies are the most diffuse type of galaxies in our modern universe and are expected to be more than one in the past. As for Cold Dark Matter (CDM), dwarf galaxies are the first to yield after Big Bang and are often thought to be the residue of the building blocks of massive galaxies [7]. Dwarfs are the most dominant type of galaxies in the universe with relatively low mass and are the regular companion of other galaxies. They are often found in clusters of galaxies [8]. There are mainly three types of dwarf galaxies: i) Spheroidal; gas-poor dwarf which is not supporting any star formations, ii) irregulars; gas-rich dwarf which supports star formation but at relatively low rates, iii) starbursting dwarf; forming star at a surprising rate [9]. Blue Compact Dwarf (BCD) is known as an irregular dwarf since it has no uniform shape. The composition of BCD is comparable to the material type during the formation of the first stars in the early universe, making it an apt object to research and understand the process of formation of the primordial stars [10].

The paper is structured as follows: the sample chosen for this study is addressed in Section II. The methods of the study was presented in Section III. Section IV contains the result and discussion part. Finally, we have concluded our results in Section V.

2. Sample Selection

We have taken two dwarf galaxies for our study namely SDSSJ222726.64+120539.8 and SDSSJ162753.47+482529.3. These galaxies are among the merging dwarf galaxies listed in the catalog of Paudel et al. [11]. SDSS J222726.64+120539.8 is positioned in the sky at R.A.: 22h 27m 26.64, Dec.: 12d 05m 39.8s with a redshift value 0.0118 whereas, SDSS J162753.47+482529.3 is located in the sky at RA.: 16h 27m 53.47s, Dec.: 48d 25m 29.3s with the redshift value 0.0134. The g & r band magnitudes of SDSSJ222726.64+120539.8 and SDSSJ162753.47+482529.3 are 15.68 & 15.65 mag, and 16.47 & 16.19 mag, respectively. The optical view of selected dwarf galaxies is shown in Figure 1. Figure 2 shows the SDSS optical spectrum of the galaxies, wavelength (for both galaxies) ranging from 4100 Å to 6700 Å. The strongest among all those emission lines are OIII and Hα in these galaxies distinctly.

3. Methods

We have analyzed the emission lines featured in the 2-D spectrum to study the properties such as line ratio, star formation rate, and metallicity of the dwarf galaxies. These images and spectrums were well-calibrated and no further reductions were required. The SDSS fibers had an arc diameter of 3 seconds. Therefore, these spectrums only cover the small area of these dwarf galaxies. We downloaded the spectrum data from the SDSS server (http://skyserver.sdss.org/dr14). The observed

emission lines from the spectrum were then studied using the software Origin8.5. The strongest emission lines, as shown in Figure 2, were then Gaussian fitted for the estimation of different statistical parameters. We also noted the parameter like FWHM, total flux, and best fits coefficients. In order to get an accurate corresponding flux of the emission line, we subtracted the continuum flux.

Fig. 1: Optical view of SDSS J222726.64+120539.8 (upper) and SDSS J162753.47+482529.3 (lower).

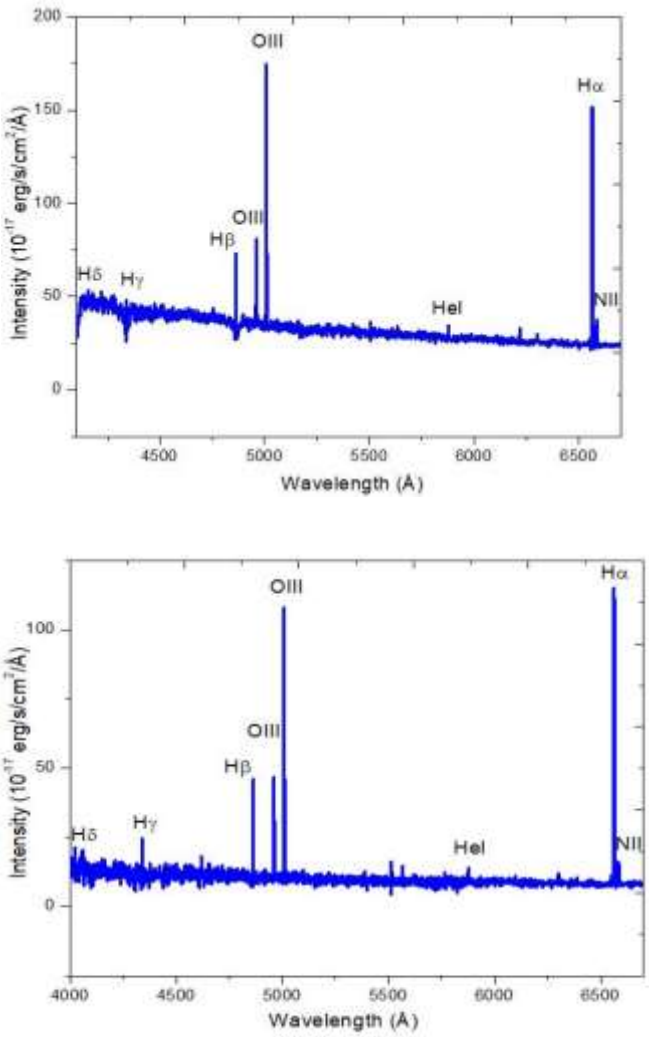

Fig.2: 2-D optical spectrum of SDSS J222726.64+120539.8 (upper) and SDSS J162753.47+482529.3 (lower) with several prominent emission lines.

The Gaussian function is defined as [12, 13]:

$$f_G(x) = \frac{1}{\sqrt{2\pi\sigma^2}} e^{\frac{-(x-\mu)^2}{2\sigma^2}}, \quad (1)$$

where, x, μ, and σ are normal random variables, mean deviation, and standard deviation respectively.

The Gaussian fitting of each emission lines studied with higher intensities and their respective FWHM, offset, and regression coefficients were tabulated and discussed in the later section. FWHM is the value at which the dependent variable is equal to half of its maximum value. Kennticutt (1998) [4]

obtained the qualitative estimation of total star formation (SFR) in the galaxies through photometry of coalescing Hα lines from a large sample of galaxies. The star formation rate can be calculated as:

$$SFR\ (M_{\odot} year^{-1}) = 7.9\times 10^{-42}\ \Sigma\ L\ (H\alpha)\ (ergs\ s^{-1}), \quad (2)$$

where ΣL(Hα) is the total luminosity of the Hα line after Gaussian fitting. Σ L(Hα) = Area of Gaussian fit × 10^{-17} × $4\pi R^2$ (ergs s^{-1}). R is the radius of the sphere and is calculated as R = D × 3.08 × 10^{24} cm. Here, D is the luminosity distance the galaxy is from the earth which is calculated using the redshift value in Mpc [13].

We used a line ratio between Hα and NII to derive the emission line metallicity given by [14],

$$12 + \log (O/H) = 8.743 + 0.462 \times \log (NII/\ H\alpha), \quad (3)$$

4. Results and Discussion

Among the various methods used to estimate the rate of star formation, we have adopted the method of Hα measurement estimated by Kennicutt, 1998, easiest, commonly used method of SFR determination as it provides estimation of SFR rate from the Hα emission lines of the spectra of the galaxies. We have analyzed the Balmer series i.e., Hα, Hβ, Hγ, and Hδ, these lines are primarily associated with the gas-mass and star formation rate in the galaxies. The other strongest emission lines like HeI, OIII, OIII, and NII were also identified to study the chemical parameters of the galaxy. The OIII is doubly ionized oxygen. Figures 3 and 4 display the example of Gaussian fits of two emission lines i.e. Hα and NII for the galaxies SDSSJ222726.64+120539.8 and SDSSJ162753.47+482529.3, respectively. The red line displays the Gaussian distribution with the error bars in the Gaussian curve. We pointed out that the data observed and the Gaussian distribution are in close agreement, which suggests the effectiveness of the findings. In the same way, we made the Gaussian fit for other emission lines as well. Tables 1 and 2 list the entire identified element with the strongest emission lines. The noted emission lines are redshift calibrated to get the corresponding emitted wavelength and are subjected to the baseline subtracted to get accurate flux. The Gaussian parameters of all eight Gaussian distributed emission lines are listed with their offset values. The average coefficient of regression was found to be 0.98.

SDSS J222726.64+120539.8

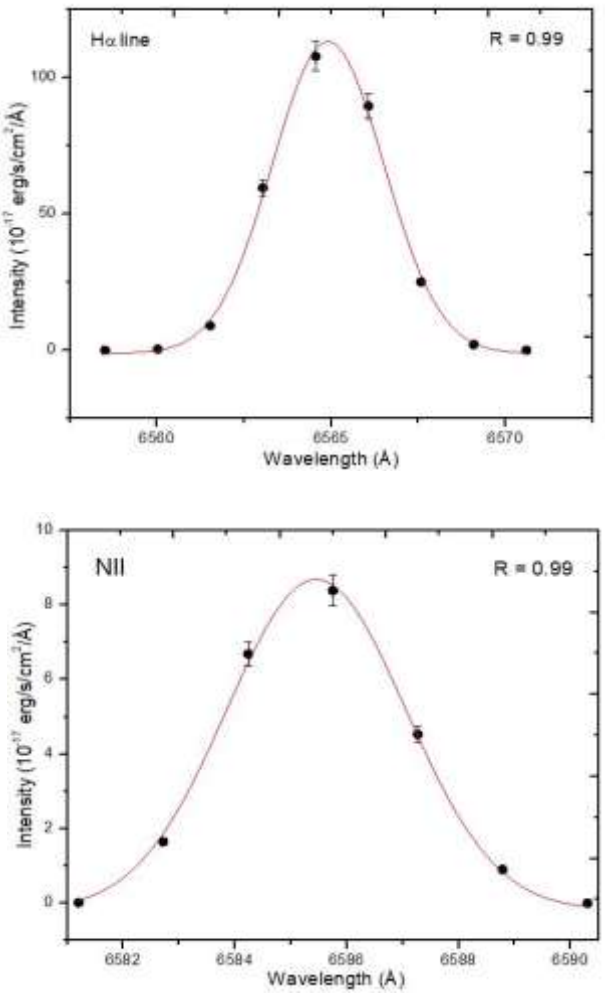

Fig. 3: Example of Gaussian fitting of two emission lines Hα (left) and NII (right) of the galaxy SDSSJ222726.64+120539.8.

From Table 1, we observed that the wavelength of 6564.63 Angstroms had the highest intensity of 113.09 x 10^{-17} erg/s/cm^2/Å corresponding to the Hα line of the Balmer series. Similarly, the second peak

had an intensity of 103.05 x 10^{-17} erg/s/cm^2/Å which corresponds to the doublet OIII lines. The intensity at 5877.24 Angstrom had a low value of 5.63 x 10^{-17} erg/s/cm^2/Å which resembles the HeI emission line. For the calculation of the star formation rate, we used the formula described in Equation 2. Redshift value (z) = 0.0118 from the catalog of Paudel et al. (2018) [11] was used to calculate the distance to the galaxy (D). We calculated the value of D as 49.17 Mpc. The star formation of the galaxy was found to be 0.010 $M_{\odot}year^{-1}$. We also estimated the line ratio of Hα and Hβ. It was found to be 2.78, which is slightly less than the theoretical value (Hα/Hβ = 2.8) [13] for the star-forming galaxies modeled by Dessauges-Zavadsky et al. [15]. The ratio of NII and Hα was used to estimate the emission line and metallicity. Metallicity indirectly traces the history of star formation, demonstrating the stability of many of the galaxies' essential physical mechanisms, such as the expulsion of metals into the ISM by supernova and stellar winds, the deportation of gas through galactic outflows, and the accretion of gas from local environments in the galaxy [16]. The physical mechanism that controls the formation of stars and, most importantly, the evolution of galaxies can be understood by analyzing metallicity evolution in relation to the other essential properties of galaxies [16]. The value of emission line metallicity, calculated using Equation 3, was found to be 8.23 dex.

Table 1: Statistical parameters obtained from the Gaussian fit of the emission lines of the spectrum of the galaxy SDSSJ222726.64+120539.8.

Emissions	Wavelength (Å)	Peak Intensities (10^{-17} erg/s/cm^2/Å)	FWHM (Å)	Area (10^{-17} erg/s/cm^2/Å)	Offset	R- Square
Hδ	4102.89	7.67	2.21	19.14	-0.113	0.97
Hγ	4341.69	18.32	2.32	47.26	-0.424	0.99
Hβ	4862.69	40.64	2.84	40.64	-0.348	0.99
OIII	4960.295	36.89	2.75	103.05	0.142	0.98
OIII	5008.24	103.05	3.01	327.83	-0.170	0.99
HeI	5877.24	5.63	3.74	23.29	0.307	0.98
Hα	6564.63	113.09	3.77	458.81	-0.319	0.99
NII	6585.27	8.68	3.77	35.63	-0.041	0.99

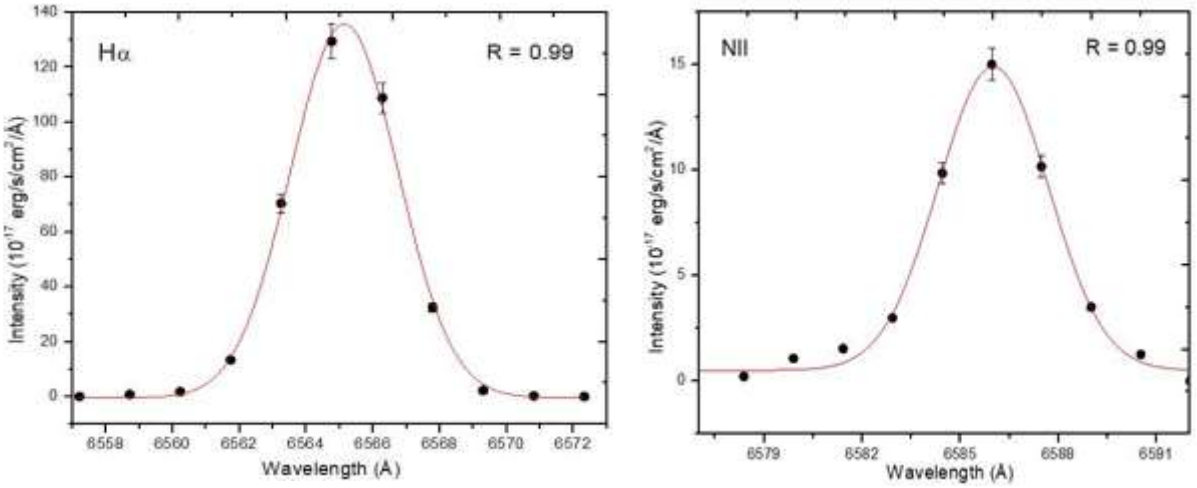

Fig. 4: Example of Gaussian fitting of two emission lines Hα (left) and NII (right) of the galaxy SDSSJ162753.47+482529.3.

SDSS J162753.47+482529.3

From Table 2, we noticed that the 4960.295 Angstrom had the highest intensity of 142.12 x 10^{-17} erg/s/cm^2/Å corresponding to the doublet OIII emission line. Similarly, the observed second peak had an intensity of 135.76 x 10^{-17} erg/s/cm^2/Å which corresponds to the Hα line. The intensity had a low value of 8.65 x 10^{-17} erg/s/cm^2/Å which belongs to the Hδ line. In a similar way as in the previous galaxy, the formula described in equation 2 was to find the star formation rate of this galaxy. The distance (D) to the galaxy was estimated to be 55.83 Mpc using redshift value z = 0.0134 [11]. The star formation rate of the galaxy was found to be 0.016 $M_{\odot}year^{-1}$. The line ratio between Hα and Hβ for this galaxy was 2.85, which is estimated to be slightly greater than the theoretical value (Hα/Hβ = 2.8), which is due to internal extinction. The emission line metallicity for this galaxy was also calculated using Equation 3 and was found to be 8.7 dex.

Table 2: Statistical parameters obtained from the Gaussian fit of the emission lines of the spectrum of the galaxy SDSSJ162753.47+482529.3.

Emissions	Wavelength (Å)	Peak Intensities (10^{-17} erg/s/cm^2/Å)	FWHM (Å)	Area (10^{-17} erg/s/cm^2/Å)	Offset	R- Square
Hδ	4102.89	8.65	2.16	26.93	-0.114	0.98
Hγ	4341.69	18.56	3.86	112.57	-0.576	0.94
Hβ	4862.69	47.64	3.08	161.71	-0.234	0.99
OIII	4960.295	46.50	2.82	142.94	0.245	0.99
OIII	5008.24	142.12	2.94	449.64	-0.113	0.99
HeI	5877.24	7.30	3.61	27.04	0.041	0.95
Hα	6564.63	135.76	3.79	549.59	0.386	0.99
NII	6585.27	14.89	3.96	60.58	0.097	0.99

5. Conclusion

In this paper, we performed the Gaussian fit of the strongest emission lines from the spectrum archived from the SDSS server of two dwarf galaxies namely SDSSJ222726.64+120539.8 and SDSSJ162753.47+482529.3 to estimate the star formation rate, line ratio of Hα and Hβ, and emission-line metallicity of the galaxies. In both of the galaxies, the FWHM value corresponding to each element was below 4 Å. This shows that the observed characteristic lines are in close agreement with Gaussian fits. Also, we calculated the star formation rate from their Hα measurement as 0.010 $M_{\odot}year^{-1}$ and 0.016 $M_{\odot}year^{-1}$(indicating low star formation rate) and the metallicity as 8.23 dex and 8.7 dex for SDSSJ222726.64+120539.8 and SDSSJ162753.47+482529.3, respectively. In the future, the star formation rate will be estimated using FUV measurement and compared with these results. In addition, a photometric study of these galaxies will be carried out in order to observe other physical and morphological properties based on previous models.

Acknowledgment

We would like to acknowledge D.N. Chhatakuli, Ph.D. Scholar, Central Department of Physics, Tribhuvan University, for sharing his knowledge in this work. His previous studies inspired us to work in this field. We are also thankful to Sanjay Paudel, Centre for Galaxy Evolution Research, Department of Astronomy, Yonsei University,

Seoul, South Korea for providing a catalog of dwarf galaxies. We extend acknowledgment to SDSS Data Server and Origin8.5.

Author contributions

This work was carried out under the guidance of the author B. Aryal. All the authors have equal contribution throughout the work.

References

[1] F. Schweizer, Colliding and merging galaxies, Science 231 (1986) 227-234. https://doi.org/10.10.1126/science.231.4735.227

[2] R. C. Kennicutt-Jr, The rate of star formation in normal disk galaxies, The Astrophysical Journal 272 (1983) 54-673. https://doi.org/10.10.1086/161261)

[3] M. M. Anđelic, Star formation rate in Holmberg IX dwarf galaxy, Serbian Astronomical Journal 183 (2011) 71-75. https://doi.org/10.2298/SAJ1183071A)

[4] R. C. Kennicutt-Jr, Star formation in galaxies along the Hubble sequence, Annual Review of Astronomy and Astrophysics 36 (1998) 189-231. https:\\doi.org/10.1146\annurev.astro.36.1.189

[5] S. Huang, M. P. Haynes, R. Giovanelli, J. Brinchmann, S. Stierwalt, & S. G. Neff, Gas, stars, and star formation in ALFALFA dwarf galaxies, The Astronomical Journal 143(6) 2012 133. https://doi.org/10.1088/0004-6256/143/6/133

[6] E. C. Elson, W. J. G. De Blok, & R. C. Kraan-Korteweg, Star formation models for the dwarf galaxies NGC 2915 and NGC 1705, The Astronomical Journal 143 (2011) 1. https://doi.org/10.1088/0004-6256/143/1/1

[7] M. Cignoni, & M. Tosi, Star formation histories of dwarf galaxies from the color-magnitude diagrams of their resolved stellar populations, Advances in Astronomy (2010). https://doi.org/10.1155/2010/158568

[8] A. H. Corporaal, Dust and Star Formation in Early-type Dwarf Elliptical Galaxies in the Fornax and Virgo Cluster (Doctoral dissertation, Faculty of Science and Engineering) (2017). http://fse.studenttheses.ub.rug.nl/id/eprint/15367)

[9] F. Lelli, F. Fraternali, and M. Verheijen, Evolution of dwarf galaxies: a dynamical perspective, Astronomy & Astrophysics 563 (2014) A27. https://doi.org/10.1051/0004-6361/201322658

[10] A. Morrow, European Space Agency (ESA), Hubble's true blue compact dwarf, https://www.nasa.gov/image-feature/goddard/hubbles-true-blue-compact-dwarf (Available online)

[11] S. Paudel, R. Smith, S. J. Yoon, P. Calderón-Castillo, and Duc PA, A catalog of merging dwarf galaxies in the local universe, The Astrophysical Journal Supplement Serie 237 (2018) 36. https://doi.org/10.3847/1538-4365/aad555

[12] X. Zhang, Gaussian Distribution. Encyclopedia of Machine Learning, Springer (2011). https://doi.org/10.1007/978-0-387-30164-8_323

[13] D. N. Chhatkuli, B. Aryal, S. Paudel, A spectroscopic study of the low redshift dwarf galaxy SDSS J134326.99+431118.7 to calculate star formation rate, BIBECHANA 18 (2021) (1) 100-107. https://doi.org/10.3126/bibechana.v18i1.29466

[14] R. A. Marino, F. F. Rosales-Ortega, S. F. Sánchez, A. G. De Paz, J. Vílchez, D. Miralles-Caballero, ... & A. I. Díaz, The O_3N_2 and N_2 abundance indicators revisited: improved calibrations based on CALIFA and Te-based literature data, Astronomy & Astrophysics 559 (2013) A114 https://doi.org/10.1051/0004-6361/201321956

[15] M. Dessauges-Zavadsky, M. Pindao, A. Maeder, D. Kunth, Classification of emission-line gal, Vizier Online Data Catalog (J/A+A) 355 (2000) 89.

[16] M. C. Cooper, C. A. Tremonti, J. A. Newman, A. I. Zabludoff, A.I, The role of environment in the mass–metallicity relation, Monthly Notices of the Royal Astronomical Society 390 (2008) (1) 245–256.